POTENTIAL OF HYPERSPECTRAL REMOTE SENSING FOR VEGETATION MAPPING OF HIGH MOUNTAIN ECOSYSTEMS

K. Bakos, P. Gamba [a]

[a] Department of Electronics, University of Pavia
{karoly.bakos, paolo.gamba}@unipv.

KEY WORDS: Hyperspectral, Vegetation mapping, Processing chain

1. ABSTRACT:

Remotely sensed data is widely used in ecological applications because of its great advantages. These advantages are that the measures are being objective, repeatable and serve continuous data of the observed area opposed to traditional field survey based data collection (Zagajewskij et al. 2005). The remote observation of different vegetation species is important and quantitative and qualitative information can be derived by interpreting satellite/airborne images (Cjemg et al 2006). With the capabilities of hyperspectral sensors theoretically the possibilities are extended to derive more information with higher level of accuracy. In vegetation mapping and monitoring unfortunately this needs more sophisticated algorithms and techniques as traditional data processing techniques developed for processing of multispectral data are often fail because of the significantly more complex nature of hyperspectral imagery. Throughout the HYPER-I-NET project we aim to further extend the application possibilities of hyperspectral datasets therefore significant effort is being made in order to develop and test methodologies useful for hyperspectral data applications. Within the project we specifically study the vegetation related aspects of hyperspectral data processing such as land cover mapping and vegetation monitoring. In this field significant amount of research can be found within the technical literature but none of them is aiming the achievement of a generally applicable methodology that is useful for generic mapping purposes. Most of the techniques presented are highly specific for the specific application and the vegetative species that are being observed and mapped.
In this paper we present the results of a comprehensive test of different hyperspectral data processing chain with the aim to identify the possibilities of moving forward to a generic data processing chain for vegetation mapping by means of hyperspectral imagery. During the research we built and tested certain data processing chains wile varying the methodologies used at different stages of the data processing system. As a following step an in-depth analysis of results were carried out aiming to find optimal solution for the given problem. The outcomes of the study shows that hyperspectral datasets can be successfully used in a generic vegetation mapping procedure but more careful design and implementation of classification system is required. Some of the standard data processing chains are selected and are being identified to be more suitable for vegetation mapping than the others.

2. INTRODUCTION AND BACKGROUND

Detection of vegetation cover serves probably the most basic information on the condition of different ecosystems and can be derived from remotely sensed data. Application of high spectral and spatial resolution hyperspectral imagery for mapping is particularly suitable for high mountain communes as in many case the traditional mapping methodologies are unsuitable because of the habitats are inaccessible (Zagajewskij et al. 2005)
This work presents the methodologies and the results of vegetation mapping using hyperspectral airborne data and field mapping techniques in high mountain ecosystems. The study also aims to give a comparison of different remote sensing classification methods and to address the possibility of using spatial and ancillary information during the image interpretation.
There are many methodologies addressing hyperspectral data processing (Cheng 2006, Guo 2006, Robila 2005) but not many studies are focused on the issue of general mapping of vegetation by means of imaging spectroscopy. The study which is the core of this research work is thus aimed at investigating the possibilities and find optimal solution regarding hyperspectral data processing chain for vegetation mapping purposes. This was done by assessing the performance of different processing chains and analysing the image interpretation results. Differently from what we have done in the past (Nairoukh et al. 2008) however, in this work the inputs to the processing chain may vary, and spatial and ancillary information has been also considered.
At first, starting from a radiometrically and geometrically corrected dataset, the performance of each step of a generic data processing chain as proposed by Gamba et al. (2007) was investigated, while different methodologies were used both for dimensionality reduction and for data classification. Feature selection and feature extraction methods include Principal Components Analysis, Minimum Noise Fraction forward rotation, Decision Boundary Feature Extraction and Discriminant Analysis Feature Extraction. For classification Maximum likelihood algorithm, Spectral Angle Mapper and Neural Network algorithms were used. In order to assess the performance of data processing while ancillary data is used the DEM and “a priori” knowledge was used and a novel multistage classifier was specifically designed. The classifier starts by discarding very steep areas and easier cover types and then goes on differentiating more difficult land cover types. To investigate the potential of spatial information within the classification procedure, the previously generated classification images were reprocessed using a spatially-aware approach based on a fuzzy neural network structure.

Moreover, as a consequence of present study generic land cover classification by means of hyperspectral imagery is suggested by using ensemble classification systems as the mapping accuracy by different techniques were found to be highly class and input source dependent. A Decision Tree (Wallace 2003) Structure is suggested for data processing where different land cover types are being mapped using an entirely different data processing chain. Finally the result of such an experimental classification system designed and implemented in a manual fashion is presented. A follow up of this research is the implementation of a multi-stage, multi-source DTC classification system that is capable to carry out data processing in a highly accurate and flexible manner and is automated.

3. STUDY AREA AND MATERIALS

The study area in this research was a high mountainous area in Poland covering the extent of the Tatra National Park with a complex vegetative coverage ranging from bare rocks over different grassland communes and associations to the densely vegetated coniferous shrubs and woodlands. Our exact study are corresponds to Gasienicowa Valley with its surroundings. The area is located between 49°13'00"E and 49°15'00"E and between 20°00'00"N and 20°03'00"N, and includes alpine and subalpine zones ranging in altitude from about 1500 to about 2300 meters above sea level. The test set used in this research was a DAIS 7915 dataset provided by the University of Warsaw in the framework of the HYPERINET (Hyper-i-net website)] project and was collected by DLR over the HySens campaign. A full coverage of field measured ground truth data was also available an additional validation data was collected during July 2008.
The Digital Airborne Imaging Spectrometer (DAIS) operated by DLR is a hyperspectral airborne sensor has its own spectral and geometric characteristic that is summarised below in a tabular format according to DLR specifications (Dlr WEBSITE).

Spectrometer Characteristics
Wavelength range: 400nm - 12.6µm, 4 Spectrometers, 79 bands
1) 400 - 1000 nm : 32 Bands, Bandwidth = 15-30 nm Detector: Si 2) 1500 - 1800 nm : 8 Bands, Bandwidth = 45 nm Detector: InSb 3) 2000 - 2500 nm : 32 Bands, Bandwidth = 20 nm Detector: InSb 3000 - 5000 nm : 1 Band , Bandwidth = 2.0 µm Detector: InSb 4) 8000 -12600 nm : 6 Bands, Bandwidth = 0.9 µm Detector: MCT The details of center wavelengths and bandwith information can be found at DLR website.
Main radiometric parameters
Dynamic range: 15 bit (no gain settings) Sensitivity VIS/NIR: NER < 0.025 mW/cm²sr µm SWIR: NER < 0.025 mW/cm²sr µm MIR/TIR: NET < 0.1 K
Main geometric parameters
FOV: 0.894 rad (+-26 degrees) on DO 228, depending on aircraft max. +- 39 IFOV: 3.3 mrad, (0.189 degrees) GIFOV: depending on aircraft altitude 5 - 20 m Scan frequency: adjustable according to aircraft altitude between 6 and 24 Hz Image pixels per line: 512

Table 1 Specification of the DAIS 7915 airborne sensor by DLR

4. METHODOLOGZ

The methodology focused on the testing of different data processing chains for classification of the hyperspectral imagery and then analyse the results of different classifications. For data processing chain definition we used the approach of Gamba et al. (2007) that consist of a two stage processing chain with different steps as illustrated in Figure 1

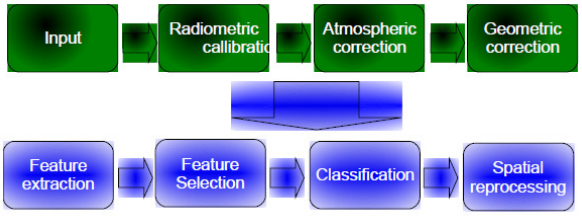

Figure 1 Generic concept of processing chain for hyperspectral data processing using Gamba et al (2007)

.

During the data processing and testing the different approaches we only focused our work on the second part of the processing chain marked with blue and tried several different approaches at each stage of it. For feature selection and feature extraction Principal Components Analysis (PCA) Jolliffe 1986], Minimum Noise Fraction Rotation (MNF) ()Green 1988, Discriminate Analysis Feature Extraction (DAFE) (Landgrebe 2003), Decision Boundary Feature Extraction (DBFE) (Lee and Landgrebe 1991)and Feature Selection algorithms based on transformed divergence (Richards 2006) were used. For classification also several supervised algorithms were used such as Maximum Likelihood (ML) (Kay 1993) classification, Spectral Angle Mapper (SAM) (Yuhas 1992) and a Fuzzy Neural Network (NN) classifier (Gamba et al. 2003). As the Digital Elevation Model (DEM) of the area was also available it was used as ancillary dataset to mask the very steep slopes of the area in order to not tot bias the classification results. Each of the previously produced transformed datasets was classified with these methodologies and accuracy measures were carried out. On the classification images generated a further attempt was made for spatial reprocessing of the results using a spatially enabled Neural Network Classifier (Li 2008) in order to further increase classification precision and the accuracy levels were assessed again. The schematic of this workflow is shown in figure 2.

The different possible processing chains are shown in figure 3 with the combination of different configurations. Also some of the overall well performing data processing approaches regarding to the dataset are highlighted. To measure the classification accuracy levels confusion matrices were used. For the identification of the well performing processing chain configurations the overall accuracy was used as the main measure, but in the analysis of different processing chains the confusion matrices were used on a per class basis. The obtained tabular results were plotted in order to be easier to compare.

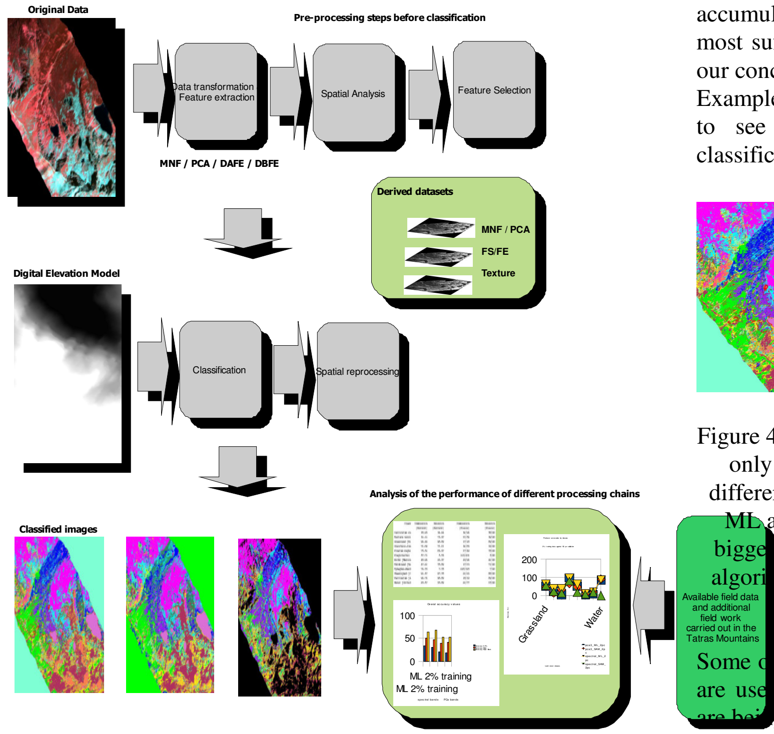

Figure 2 The workflow of the project. Starting with the original hyperspectral dataset the different processing steps were carried out and finally the results were analysed and compared in order to obtain sufficient information on how the hyperspectral data classification accuracy depends on the processing steps applied on the data.

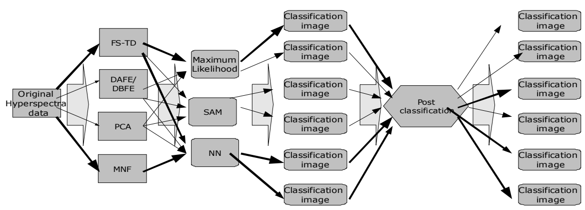

Figure 3 Graphical representation of the approach applied to while designing the different processing chains. Paths with highlighted arrows are identified to be more suitable than others. (FS-TD=Feature selection with transformed divergence; MNF=Minimum noise fraction rotation; PCA=Principal components rotation; SAM=Spectral angle mapper; NN=Neural Net).

5. RESULTS

The results obtained in this work are a series of land cover maps and classification results that belong to a certain processing chain and processing methodology and the interpretation of them. Examples of classification results and most relevant confusion matrices are presented below. As high number of classifications were carried out the entire set of classification results are exceeding the limits of present paper therefore only most relevant confusion matrices and accumulated results can be presented that are found to be most sufficient to represent the obtained results and support our conclusions.

Examples of the obtained classifications are shown in order to see the differences arisen from applying different classification chains in order to interpret the same dataset.

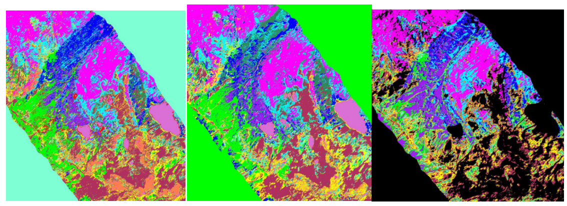

a b c

Figure 4 Examples of classification images. The examples are only shown in order to show the differences among the different processing chain results. a, shows the result of the ML algorithm, b, shows that the NN algorithm obtained bigger chunk of land cover patches and c, shows the SAM algorithm result where the black area is unclassified due to that SAM could not label those pixels.

Some of the confusion matrices are presented as a whole that are useful to understand the conclusions of the project and are being referred to in the interpretation of the results.

In order to be easier to interpret the results the most important interpretation results are summarized in tables where only the overall accuracy is used as the measure of efficiency of the classification system. This is done because the analysis of each confusion matrices obtained during the classifications would exceed the frames of present papers. The most promising results were obtained using the ML and the NN algorithms with different input sources while SAM results are shown to prove the underperforms of the algorithm when lot of complex classes are introduced for the classification system.

Class	Caricetum	Festuca versicoloris	Grassland	Oreochloo	Pinetum mugi	Pogiotechio	Rocks	Shrubland	Sphagno	Unassigned	Vaccinetum	Water	Total
Unclassified	0	0	0	0	0	0	0	0	0	0	0	0	0
Caricetum	60	3	4	4	0	0	0	2	2	3	4	1	83
Festuca versicoloris	7	40	9	15	4	0	5	0	2	10	9	0	101
Grassland	3	7	33	2	15	1	2	11	6	12	19	1	112
Oreochloo-Jun	0	6	0	26	1	0	10	4	0	12	6	0	65
Pinetum mugi	1	0	1	4	30	5	3	15	3	4	9	1	76
Pogiotechio	4	0	3	1	29	81	1	1	1	2	1	0	124
Rocks	0	7	3	23	3	1	51	6	0	13	12	2	121
Shrubland	0	2	0	1	0	0	5	42	0	2	2	2	56
Sphagno	11	17	36	1	4	1	4	9	76	16	13	0	188
Unassigned	0	0	0	7	3	0	5	0	0	8	6	3	32
Vaccinetum	4	8	1	6	1	1	3	0	0	6	9	1	40
Water	0	0	0	0	0	0	1	0	0	2	0	79	82
Total	90	90	90	90	90	90	90	90	90	90	90	90	1080

Table 2 MNF rotated image Confusion matrix of the Maximum Likelihood classification of the dataset were classification input is the

Class	Carricetum	Festuca versicoloris	Grassland	Oreochloo	Pinetum mughi	Plagiotechio	Rocks	Shrubland	Sphaghno	Unassigned	Vaccinetum	Water	Total
1 Unclassified	59	53	51	75	53	25	81	77	33	59	65	14	646
2 Carricetum	0	23	0	0	0	0	0	0	0	0	0	0	23
3 Festuca versicoloris	24	0	16	9	3	0	3	1	19	12	14	0	101
4 Grassland	1	2	7	0	3	0	0	3	5	1	3	0	25
5 Oreochloo	0	0	0	0	0	0	0	0	0	1	0	0	1
6 Pinetum mughi	2	0	6	0	16	13	0	7	2	4	2	0	54
7 Plagiotechio	0	0	0	0	13	50	1	0	0	1	0	0	65
8 Rocks	0	0	0	2	0	0	4	0	0	3	2	0	11
9 Shrubland	1	0	0	0	0	0	0	0	3	0	0	0	4
10 Sphaghno	0	3	10	0	0	0	1	2	28	6	3	0	53
11 Unassigned	0	0	0	0	0	0	0	0	0	0	0	0	0
12 Vaccinetum	3	9	0	4	0	1	0	0	0	1	1	1	20
13 Water	0	0	0	0	0	0	0	0	0	2	0	75	77
Total	90	90	90	90	90	90	90	90	90	90	90	90	1060

Table 3 Confusion matrix of the SAM classification of the MNF rotated image

Class	Carricetum	Festuca versicoloris	Grassland	Oreochloo	Pinetum mughi	Plagiotechio	Rocks	Shrubland	Sphaghno	Unassigned	Vaccinetum	Water	Total
Unclassified	0	0	0	0	0	0	0	0	0	0	0	0	0
Carricetum	61	2	5	7	1	0	3	2	5	3	4	2	95
Festuca versicoloris	10	54	8	18	3	0	5	1	8	15	12	0	132
Grassland	2	4	24	1	12	0	2	6	3	12	14	0	80
Oreochloo	1	4	1	15	2	1	13	5	0	8	10	2	62
Pinetum mughi	2	0	6	4	29	4	7	8	5	8	7	0	80
Plagiotechio	0	0	4	1	32	82	0	2	0	4	2	0	127
Rocks	0	4	0	22	1	0	45	6	0	8	8	2	98
Shrubland	5	2	2	4	4	0	2	47	5	4	5	2	82
Sphaghno	7	14	33	1	1	0	1	8	64	14	8	0	151
Unassigned	0	1	6	12	4	1	6	1	0	10	8	4	53
Vaccinetum	0	5	1	7	1	2	6	4	0	2	12	3	43
Water	2	0	0	0	0	0	0	0	0	2	0	75	79
Total	90	90	90	90	90	90	90	90	90	90	90	90	1060

Table 4 Confusion matrix of the ML algorithm applied on the feature selected (Transformed divergence based) input data source

Class	Grassland	Festuca	Oreochloo	Pinetum	Plagiotechio	Rocks	Shrubland	Spagiotechio	Vacinatum	Water
Unclassified	c	0	0	0	0	0	0	0	0	0
Festuca	80	0	2	0	0	0	0	0	2	0
Grassland	0	78	0	4	0	0	0	0	8	0
Oreochloo	5	1	73	7	1	9	3	0	7	4
Pinetum mughi	0	3	0	65	6	2	9	0	1	0
Plagiotechio	0	0	0	9	83	1	0	0	0	0
Rocks	1	1	11	1	0	71	0	1	4	0
Shrubland	0	0	0	4	0	0	78	0	0	0
Spagiotechio	0	4	0	0	0	0	0	88	0	0
Vacinatum	4	3	4	0	0	7	0	1	68	0
Water	0	0	0	0	0	0	0	0	0	86
Total	90	90	90	90	90	90	90	90	90	90

Table 5 Classification results of the MNF image into 11 classes using Maximum Likelihood algorithm

The overall accuracy levels of most of the tested processing chains were found to be sufficient for land cover mapping. The results are shown in the table below and it can be seen that the overall well performing chains gained similar classification results in terms of overall accuracies. The accuracies shown below are representing the overall accuracy level measured on the classifications using 9 classes of the ground truth map where underrepresented classes were merged into the most appropriate class based on physiological and phonological properties.

Methodology	Accuracy (%)
FS – ML Classificaiton	81,38%
FS – SAM Classification	57,77%
FS – PCA – ML Classification	72,08%
FS – DAFE – ML Classification	72,08%
FS – DBFE – ML Classification	74,58%
FS – Fuzzy Neural Net	79,23%

Table 6 Classification accuracy levels of some of the well performing processing chains

The spatial reprocessing of the classification images are in most case further increased the interpretation accuracy by eliminating errors originated from misinterpretation of pixels. The most relevant results are shown in the table below.

Dataset and Methodology	Overall accuracy without reprocessing (%)	Overall accuracy after reprocessing (%)
Algoorithm: ML Input: MNF 15 Band Spatial proc.: Adaptive bit error	84,1111	84.2121
Algoorithm: NN Input: MNF 15 Band Spatial proc.: NN	87,66	87,77
Algoorithm: ML Input: Spectral 10 Band Spatial proc.: NN	81,38	87.96

Table 7 Classification accuracy levels of some of the well performing processing chains and the results after the spatial reprocessing of the classification image

6. DISCUSSION

In summary, we found that regarding to our dataset there were certain processing chains that were found to be superior to others when the obtained overall accuracy of the classification is used as the main measure of how successful an interpretation procedure is. However when analyzing the different confusion matrices obtained during the classifications it can be seen that the accuracy levels are varying not just based on the methodology used for classification but also correlate to the actual class that is mapped. With other words although there are generally well performing processing chains some of the classes can be detected more successfully when a processing chain is used that performs on low level in general.

6.1 Data dimensionality reduction

The performance analysis of different processing chains showed that for data dimensionality reduction the Minimum Noise Fraction forward rotation is the most powerful methodology in most cases. It outperformed Principal Components Analysis and also DAFE and DBFE. The difference among PCA and MNF was also investigated by plotting the data distribution and data values as means and standard deviation and also by classes after they were projected into the new feature spaces. Examples of such plots are shown below.

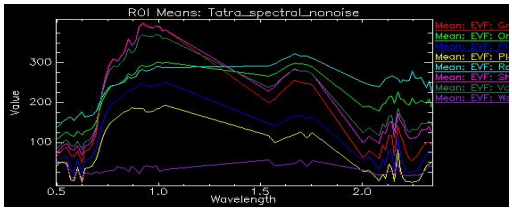

a

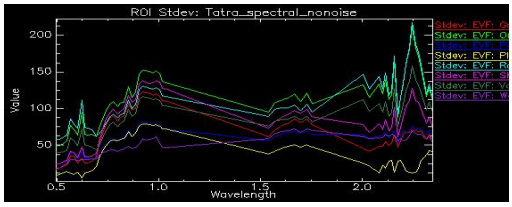

b

Figure 5 Mean values (a) and standard deviation (b) of the mean of the original spectral dataset.

Dsfasd

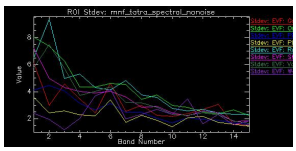

a

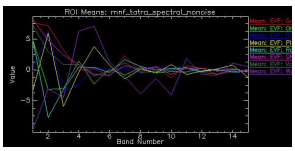

b

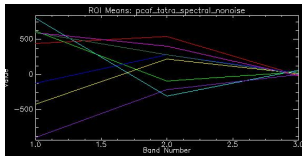

c

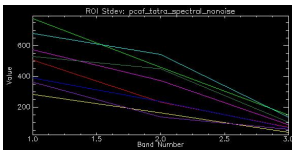

d

Figure 6 The Mean values and of PCA (a) and MNF (c) input sources and the standard deviation of the mean for PCA (b) and MNF (d).

When plotting the same values on a per class basis the difference between PCA and MNF transformation is easier to follow. Some of these examples are provided below where comparison can be done among the different data distributions after rotating the feature space. For plotting the histograms a buffered version of the available ground truth map was used therefore the number of samples is unequal.

Spectral

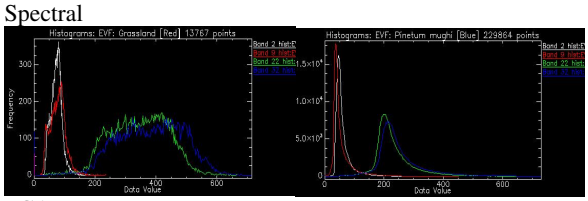

PCA

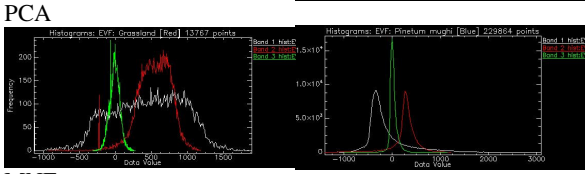

MNF

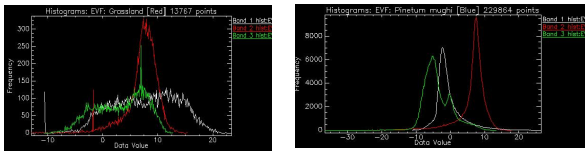

a, b,

Figure 7 The comparison of Grassland (a) and Pinetum (b) land cover types' data distribution in the original dataset, in the 1st 3 bands of the PCA projected and in the 1st 3 bands of the MNF rotated image using the histograms extracted by training dataset.

On the figures it can be seen that using the MNF rotation first of all the data is better compressed and secondly the distribution of the values is also compressed causing smaller deviation of the values of the mean. As a further consequence that can be seen in the example of the grassland land cover type plots even if grassland contains more individual land cover classes (partly that is why there are multiple peaks in the histogram) the deviation of the curve is significantly smaller in case of MNF rotated bands. This unique feature and its positive effect on classification accuracy values is supported by the selection of processing chains where in most cases MNF rotation was the data transformation technique.

Data **classification**

While analyzing the results obtained by different data processing chains the confusion matrices were exported into graphs for better visualization and comparability purposes. To produce these graphs, a large number of training and validation data was used. This results lower accuracy measures but serves better information on overall tendencies. These plots helped to identify some key elements of the differences among the different processing chains. Some examples of those plots are provided below with the aim of supporting the leveraged properties of certain processing chain configuration.

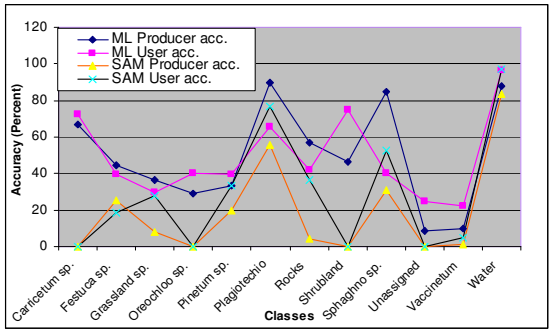

Figure 8 Comparison of user- and producer accuracy levels of two classification of the MNF rotated input data source. As can be seen on the diagram even if SAM was found to be perform poorly in overall compared to other classification methods in case of Spaggiotechio sp. The user accuracy level was higher than with ML classification that in overall served one of the best classification result.

The classification results were also analysed to see the effect of the varying input source of the classification procedure. Graphs were produced to make it easier the comparison of different classification results some of which is presented below for illustration.

Also the input of the classification was found to be affective on classification results when examining on a per pixel basis. This means that even MNF rotated image was identified to be the most suitable for a generic vegetation classification procedure the detection of some particular land cover classes (e.g. Plagiotechio sp.) gained better results when using the PCA image or the feature selected spectral bands as input source for the classification.

When we take into account the effects of the aggregation of classes that is the case when no representative field data is available the differences become more significant because the omission and commission properties of each cover types are highly depend on the transformation that was applied to the original data. This means that when classes are aggregated the classifier become more sensitive for the input data when examining on a per class bases. This is also represented in a figure where we clumped land cover classes simulating a real life situation when in the field data there is no sufficient information on underrepresented land cover classes.

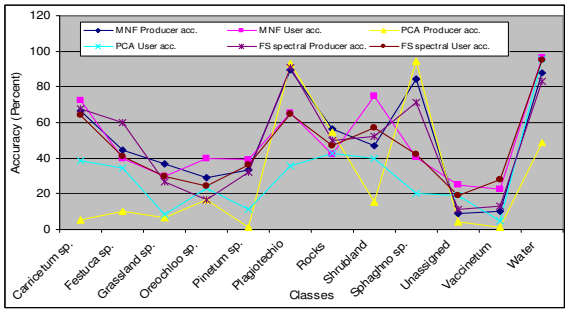

Figure 9 Comparison of classification results using the same input data source for classification and different classification methodology.

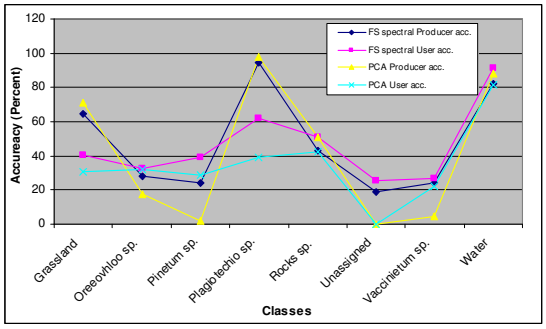

Figure 10 Producer and user accuracy levels of different classifications where input data source is changed and training data is aggregated into 8 classes.

In order to retrieve further details on the nature of classifiers a visual assessment of classification images were done. The purpose of this was to compare the classification image with each other and also with the data collected during the field survey. It was important because even if full ground truth validation data was available the accuracy of the dataset was unknown and the data was created using satellite and aerial photo interpretation but in many cases surrogate datasets were used instead of ground collected data. By the visual comparison the some of the land cover patches were linked against images taken during the field survey where the assessment of fragmentation level of ground cover polygons were emphasised. By comparing different classification images it was aimed to identify these differences among the different results.

6.2 Spatial reprocessing

By reprocessing spatially the images using a neural network approach it was aimed to remove individual pixel label errors from the classification by examining the surroundings of each pixel and train the neural network with training data in order to be able to analyse the neighbourhood area of each pixel. This means that if all surrounding pixels within a certain distance had a particular label the given pixel label was likely to be changed too that label if in the training data there were no individual pixels or small polygons present. The illustration can be seen in figure below.

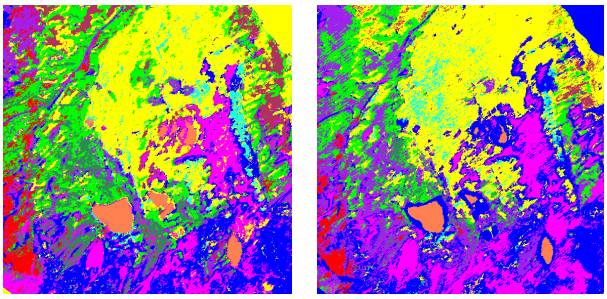

a b

Figure11 Illustration of how spatial re-processing can eliminate individual pixel classification errors. The original classification (a) and after re-processing (b)

The results showed that the spatial reprocessing of the image enabled the accuracy level to further increase. Although the increment cannot be showed really in the overall accuracy of the classification as the limited number of pixels used for assessment are not able to express the changes as they are. However in terms of overall accuracy levels a small increment can be seen. Also by visual assessment of the classification images compared to the spatially reprocessed ones showed evidence that significantly less individual pixels were labelled differently than the majority found surrounding area that resulted a more smooth classification image. Although the assessment of accuracy was found to be difficult to carry out on the spatially reprocessed images it was found that for some particular applications this result may be more appropriate than the ones without spatial reprocessing.

7. CONCLUSIONS

The processing of hyperspectral data for vegetation related applications is still an issue to be solved. The complexity of the dataset and the varying nature of vegetation land cover needs sophisticated methodologies for interpret correctly. In this study we compared different processing chains for data interpretation aiming a generally applicable data processing chain when vegetation is to be detected. In our study we found that there are some processing chains that outperform others in terms of the gained overall accuracy levels. In particular best results could have been obtained (87,66%) when the Minimum Noise Fraction forward rotation was used for data dimensionality reduction and the first 15 band of MNF image was classified using a fuzzy Neural Network algorithm. We obtained the second best results when in the same processing chain we swapped the classifier with a Maximum Likelihood algorithm, where although the overall accuracy was only 84,11% the processing time needed is significantly less. The comparison and analysis of results on a per pixel basis showed that although Spectral Angle Mapper performed poorly in terms of obtained overall accuracy level (57,77) there were some classed could be detected most accurately using this algorithm. Also the comparison of different data dimensionality techniques and the data histogram of training data after data transformation showed that the performance of techniques are slightly class dependent. Further problem identified is the huge variation of vegetation land cover's spectral reflectance properties that is constantly varying over different time scales. The reflectance is varying over a day according to biophysical processes within the plants that reacts for the incoming light amount and quality and also there is a variation over the vegetative period as the plant grows the reflectance properties are also changing. These considerations suggest that there is no single processing chain that is always going to perform with the highest overall accuracy level instead there are processing chains that are less sensitive for these variation. It can be expected that non-parametric decision rules will serve more accurate classification result while by careful pre-processing parametric classifiers can also perform on a high accuracy level.

To handle the problem of these variations and the differences arisen in classification accuracies on a per class basis we propose a flexible data processing approach by using multi stage classification system, where there is a possibility to change the applied methodology at each stage of the classifier. We suggest the application of a decision tree structure adapted for the problems of vegetation monitoring and detection by means of hyperspectral images. As a follow up of this study we examine the possibility of constructing a decision tree structure based classification system that is flexible enough and can serve high classification accuracy

level by integrating the advantages of each classifier and data dimensionality reduction technique and classification methodology.

We also suggest further studies on spatial information content of the image scenes that can also be integrated into the classification. Vegetation texture and spatial properties of the land cover seems to improve classification accuracy level. Furthermore textural information caries less over the different time scales therefore sometimes is more useful than the huge amount of spectral information of the vegetation that is observed.

We see great possibilities of hyperspectral datasets in mapping procedures therefore our future work will focus on the above problems and we will aim to further improve the generic vegetation monitoring and classification possibilities of hyperspectral data applications.

8. REFERENCES

X. Cheng, Y. Tao, Y.-R. Chen, X. Chen, "Integrated PCA-FLD method for hyperspectral imagery feature extraction and band selection", Proc. of the 3rd IEEE International Symposium on Biomedical Imaging: Nano to Macro, pp. 1384–1387, 6-9 April 2006.

DLR German Aerospace Center website, DAIS 7915 specification found at http://www.op.dlr.de/dais/dais-scr.htm visited on 25th February 2009

P. Gamba, P. and F. Dell'Acqua: Improved multiband urban classification using a neuro-fuzzy classifier, International Journal of Remote Sensing, Vol. 24, n. 4, pp. 827-834, Feb. 2003.

P. Gamba, A.J. Plaza, J.A. Benediktsson,J. Chanussot, J., "European perspectives in hyperspectral data analysis", proc. of the 2007 IEEE International Geoscience and Remote Sensing Symposium, pp. 4794-4797, 23-28 July 2007.

Green A., M. Berman, P. Switzer, and M. D. Craig, ``A transformation for ordering multispectral data in terms of image quality with implications for noise removal," IEEE Trans. Geosci. Remote Sensing, vol. 26, no. 1, pp. 65-74, 1988

B. Guo, S.R. Gunn, R.I. Damper, J.D.B. Nelson, "Band Selection for Hyperspectral Image Classification Using Mutual Information", IEEE Geoscience and Remote Sensing Letters, vol. 3, no. 4, pp. 522–526, Oct. 2006.

Hyper-I-Net website at www.hyperinet.eu visited on 21th March 2009

Jolliffe I. T., Principal Component Analysis. 1em plus 0.5em minus 0.4em New York: Spriger Verlag, 1986.

Kay, Steven M. (1993). Fundamentals of Statistical Signal Processing: Estimation Theory. Prentice Hall. pp. Ch. 7. ISBN 0-13-345711-7

D. A. Landgrebe Signal Theory Methods in Multispectral Remote Sensing John Wiley & SonsWiley-IEEE, 2003 ISBN 0471721255, 9780471721253

C. Lee and D. A. Landgrebe, "Decision boundary feature selection for nonparametric classifiers," inProc. SPSE's 44th Ann. Conf.1991, pp. 475-478.

Z. Li Fuzzy ARTMAP based Neurocomputational Spatial Uncertainty measures Photogrammetric Engineering and Remote Sensing 2008 December

Richards, John A., Jia, Xiuping, 2006, Remote Sensing Digital Image Analysis An Introduction 4th ed. pp 275

S.A. Robila, A.Gershman, "Spectral matching accuracy in processing hyperspectral data Signals", Proc. of the 2005 International Symposium on Circuits and Systems, vol. 1, pp. 163-166, 14-15 July 2005.

C. S. Wallace & J. D. Patrick, Coding Decision Trees, Machine Learning, 11, pp.7-22, 1993.

Yuhas R. H., A. F. H. Goetz, and J. W. Boardman, ``Discrimination among semi-arid landscape endmembres using the spectral angle mapper (SAM) algorithm," in Summaries of the 3rd annu. JPL Airborne Geosci. Workshop, R. O. Green, Ed. Publ., 92-14, vol. 1, 1992, pp. 147-149.

B. Zagajewski, A. Kozlowska, M. Krowczynska, M. Sobczak and M. Wrzesien, "Mapping high mountain vegetation using hyperspectral data", EARSeL eProceedings, vol. 4, no. 1, 2005.